INTERNATIONAL JOURNAL OF AGRICULTURE & BIOLOGY
ISSN Print: 1560–8530; ISSN Online: 1814–9596
24–0067/2024/32–3–249–260
DOI: 10.17957/IJAB/15.2199
http://www.fspublishers.org

Full Length Article

Characteristics of Xanthorrhizol Rich Extract from *Curcuma xanthorrhiza* in the Choline Chloride-Based Natural Deep Eutectic Solvents: DNA Protective Activity and Toxicity Profiles

Adelina Simamora[1,2,3], Kris H. Timotius[2], Heri Setiawan[3,4], Ratih A. Ningrum[3,5] and Abdul Mun'im[3,6*]
[1]*Graduate Program of Pharmaceutical Sciences, Faculty of Pharmacy, Universitas Indonesia, Depok 16424, West Java, Indonesia*
[2]*Department of Biochemistry, Faculty of Medicine and Health Sciences, Krida Wacana Christian University, Jakarta 11510, Indonesia*
[3]*National Metabolomics Collaborative Research Center, Faculty of Pharmacy, Universitas Indonesia, Depok 16424, West Java, Indonesia*
[4]*Department of Pharmacology, Faculty of Pharmacy, Universitas Indonesia, Depok 16424, West Java, Indonesia*
[5]*Research Center for Genetic Engineering, Research Organization for Life Sciences and Environment, National Research and Innovation Agency (BRIN), Cibinong 16911, Bogor, West Java, Indonesia*
[6]*Department of Pharmacognosy-Phytochemistry, Faculty of Pharmacy, Universitas Indonesia, Depok 16424, West Java, Indonesia*
[*]For correspondence: munim@farmasi.ui.ac.id
Received 05 February 2024; Accepted 28 May 2024; Published 26 July 2024

Abstract

Xanthorrhizol, a bioactive compound with different health benefits, is present in the rhizomes of *Curcuma xanthorrhiza* in abundance. In this work, natural deep eutectic solvent (NADES) based on choline chloride (CC) and organic acids (lactic acid, malic acid, and citric acid) were used as green solvent alternatives to organic solvents to extract xanthorrhizol from *C. xanthorrhiza*. CC-based NADESs and xanthorrhizol extracts were characterized. Three different native NADES were applied in this study, namely choline chloride-citric acid (CC-CA), choline chloride-malic acid (CC-MA), and choline chloride-lactic acid (CC-LA). The antioxidant, DNA damage protective, and toxicity activities were investigated. The results showed that all NADES were more polar than ethanol. All NADES were viscous and had density more than water and ethanol. The FTIR studies confirmed the formation of hydrogen bonds between the two components (choline chloride and organic acids). Due to its lowest viscosity, CC-MA was selected for xanthorrhizol extraction. HPLC analysis showed that extraction using CC-MA obtained similar amounts of xanthorrhizol and curcuminoids. NADES and their extracts showed DPPH radical scavenging and Fe^{3+} reducing activities. Although weaker than ethanol extract, all solvents and their extracts mitigated H_2O_2-induced oxidative damage to pBR322 plasmid DNA. Based on a real-time bacterial assay, all NADES and their extracts were benign to *Staphylococcus aureus*. However, NADES were more active against *Escherichia coli*, although their respective extracts are less toxic to *E. coli*. In conclusion, CC-MA NADES is the novel green extraction solvent for xanthorrhizol. Its low toxicity allows for potential application as a protective DNA damage agent.

Keywords: Antioxidant; DNA protection; NADES; Scanning electron microscopy; Toxicity

Introduction

Curcuma xanthorrhiza (family Zingiberaceae) is a valuable Indonesian medicinal plant with various health-promoting properties. Its rhizomes have been used for generations as one of the ingredients in jamu formula to treat different health issues, including constipation, hemorrhoids, fever, liver diseases, and appetite booster (Rahmat *et al*. 2021). It possesses terpenoids and phenolic bioactive compounds, including xanthorrhizol. A body of literature has reported the anticancer, antibacterial, antidiabetic, and protective pharmacological activities of xanthorrhizol on the liver and kidney (Oon *et al.* 2015; Simamora *et al.* 2022). Researchers have used conventional methods of maceration, percolation, and Soxhlet extraction using organic solvents (methanol, ethanol, acetone and hexane) to obtain *C. xanthorrhiza* extract with suitable biological activities. Ethanol maceration is the recommended method by the Indonesian Herbal Farmakope (Kesehatan 2017). These extraction processes are time- and labor-consuming and incompatible

To cite this paper: Simamora A, KH Timotius, H Setiawan, RA Ningrum, A Mun'im (2024). Characteristics of xanthorrhizol rich extract from *Curcuma xanthorrhiza* in the choline chloride-based natural deep eutectic solvents: DNAprotective activity and toxicity profiles. *Intl J Agric Biol* 32:249–260

with thermolabile compounds. (Mangunwardoyo and Usia 2012; Salea *et al.* 2014; Nurcholis *et al.* 2018).

As an alternative and environmentally friendly extraction method, green extractions are recently introduced to extract bioactive compounds to replace hazardous organic solvents. In general, deep eutectic solvents (DES) are mixtures of two or more components with specific molar ratios with lower melting points upon mixing than their constitutive components (Florindo *et al.* 2019). NADES is a subset of DES with components that are natural metabolites derived from plants. Compared to organic solvents, NADES possesses many desirable properties, including its non-flammability, low volatility, high thermal and chemical stability, wide polarity range, low vapor pressure, low cost of preparation, and readily accessible starting components (Radošević *et al.* 2016).

Previous studies reported the use of NADES for the extraction of different bioactive compounds, including phenolic compounds, anthocyanins, flavonoids and curcuminoids (Cui *et al.* 2018; Bi *et al.* 2020; Ahmad *et al.* 2021; Patil *et al.* 2021), thus showing the potential of NADES for ready-to-use plant extracts for human consumption. Previously, our study revealed that NADES with two components (glucose and lactic acid: 1:3) was suitable for extraction of xanthorrhizol from rhizomes of *C.xanthorrhiza* (Simamora *et al.* 2023). In the present study, we explore using choline chloride instead of glucose as NADES for xanthorrhizol extraction. NADES must be well characterized—including their physicochemical properties (polarity, viscosity and density) and biological activities, such as antioxidant, DNA protective and toxicological activities.

This study aimed to apply selected choline chloride-based NADES (CC-NADES) for extraction of xanthorrhizol from *C. xanthorrhiza*. For this purpose, choline-chloride (CC) was mixed with lactic acid (LA), malic acid (MA) and citric acid (CA). The mixtures without or with extracts of *C. xanthorrhiza*, were examined for their physicochemical properties (polarity, viscosity and density) and bioactivities (antioxidant, DNA protective and toxicological activities). We would then compare the effectiveness of choline chloride NADES in extracting xanthorrhizol. In this study we compare with ethanol extraction as standard for xanthorrhizol extraction from rhizome of *C. xanthorrhiza*.

Materials and Methods

Chemicals and reagents

Choline chloride (CC) was purchased from Xi'an Rongsheng Biotechnology (Xi'an, China). 2,2-diphenyl-1-picrylhydrazyl (DPPH), Lactic acid (≥ 85%), DL-malic acid (≥ 99%), Citric acid (> 99.5), Nile red and 2,4,6- tris (2-pyridyl)-s-triazine (TPTZ) were obtained from Sigma Aldrich (St. Louis, MO, USA). pBR322 DNA was obtained from BioLabs (New England, USA), GelRed nucleic acid gel staining 10.000x was obtained from Biotium (Fremont, USA). Tris-Acetate EDTA buffer 10x and Tris-EDTA buffer (pH 8) ultrapure grade were bought from Vivantis (Selangor, Malaysia). Bromophenol blue buffer dye was purchased from Geneaid Biotech (New Taipei city, Taiwan).

Plant material

Rhizomes of *C. xanthorrhiza* were collected in December 2021 from Balittro (Research Institute for Herbs and Spices), Bogor, Indonesia. A voucher specimen (voucher number: B-609/V/DI.05.07/3/2022) was deposited in the Herbarium Bogoriense, Bogor, Indonesia. The plant was identified by the Centre for Biosystematics Research and Evolution, Bogor, Indonesia.

NADES preparation and characterization

The CC-based NADES used in this study were prepared by heating and stirring. The constituting components were weighed using molar ratios (Table 1). The mixture was heated to 70°C and stirred constantly to obtain a clear and homogenous eutectic mixture. Water was added (25%, v/v), and the mixture was stirred for another 30 min. The NADES obtained were kept in a closed bottle stored at ambient temperature.

Determination of NADES physicochemical properties

The viscosity of CC-based NADES was measured at room temperature, using an Anton Paar ViscoQC 300 viscometer (Austria). A DG26 spindle type was used which was run for 30 s at 300 RPM. The density of the prepared NADES was determined by weighing 1 mL of each NADES using an M214Ai BEL analytical balance (Monza, Italy). Measurements were conducted in three replicates.

The polarity of NADES was evaluated using Nile red (9-diethylamino-5-benzo[a]phenoxazinone) as an indicator, as described previously (Jurić *et al.* 2021). The Nile red solvatochromic probe stock solution was prepared in ethanol (0.001 g/L) and NADES (980 μL) was added with 20 μL of Nile red stock solution in a 1 cm quartz cell. Maximum absorbance was determined in the visible region (400 – 750 nm) by a Libra S22 spectrophotometer. The molar transition energy was calculated using the following formula (Craveiro *et al.* 2016):

$$E_{NR}\ (\text{kcal mol}^{-1}) = 28591/\lambda_{max} \quad \text{(Equation 1)}$$

All measurements were performed in three replicates at ambient temperature.

FTIR Analysis

Infrared spectra of CC-based NADES and their starting components were recorded at room temperature on an FTIR

spectrophotometer (Agilent Cary 630, Santa Clara, USA), operated in an attenuated total reflectance (ATR) mode. The spectral range for the measurement was 400 – 650 cm^{-1}, with a spectral resolution of 4 cm^{-1} and an accumulation of 64 scans.

Extraction of *C. xanthorrhiza*

Ethanol extraction of *C. xanthorrhiza*: For comparison, extraction by ethanol was performed following a recommended method in the Farmakope Herbal Indonesia (2017). Rhizome powder was macerated in ethanol (96%) in a 1:10 ratio. After 24 h, the supernatant was separated by filtration, and the macerate was re-macerated twice using half the volume used in previous maceration. All filtrate was pooled and evaporated under reduced pressure in a Rotary vacuum evaporator (R300-Buchi, Flawil, Switzerland) to obtain dry crude extract. It was kept at 4°C until further examination.

Ultrasound-assisted extraction of *C. xanthorrhiza* with NADES

CC-based NADES extraction was performed in ultrasonic bath (Bandelin Sonorex Digitec, Berlin, Germany). Rhizome powder was blended with NADES in a flask in a 1/15 solid to liquid ratio. The mixture was sonicated for 20 min at 40°C (40 kHz), thereafter was centrifuged at 7000 RPM for 10 min. The supernatant was obtained by filtering the mixture through a Whatman filter paper (No. 1). It was kept at 4°C away from the light until further biological activity examinations.

HPLC analysis of xanthorrhizol in extract

Chromatographic analysis of xanthorrhizol and curcuminoids was conducted using an HPLC method as previously described (Simamora *et al.* 2023). Separation was performed using a C18 column (150 mm x 4.6 mm, 5 µm, Zodiac life science, Hyderabad, India). Solvent A (acetonitrile) and B (0.07% (v/v) formic acid in water) were used as a mobile phase, with a flow rate of 0.6 mL/min. Xanthorrhizol and curcuminoids were separated using a gradient elution as follows, 0–5 min, 45–50% A; 5–10 min, 50–55% A; 10–25 min, 55–60% A, 25–35 min, 60–65% A, 35–45 min, 65–70% A, 45 – 60 min, 70–100% A and 60–65 min 100% A. Xanthorrhizol was identified at 275 nm, whereas curcumin, demethoxycurcumin and bisdemethoxycurcumin at 425 nm. The linearity range for xanthorrhizol was 5–400 µg/mL, and for curcumin, demethoxycurcumin and bisdemethoxycurcumin were 2.5–100 μg/mL).

Surface morphology characterization

Scanning electron microscopy (SEM) images of rhizome powder and macerates were obtained using a Jeol JSM-IT200 SEM equipment. Samples of rhizome macerate were dried and coated with a thin layer of gold. The measurement used 20 kV accelerating voltage.

Determination of antioxidant activity of NADES and NADES extracts

DPPH radical scavenging assay: The ability of NADES and NADES extracts to scavenge free radicals was assayed using DPPH radical scavenging method, according Simamora *et al.* (2023). Fifty µL of samples were serially diluted in methanol and was added with 80 µL of DPPH solution (0.06 m*M*). The mixture was shaken for 30 min at 25°C in a microplate shaker/incubator at 300 rpm (Thermostar BMG Labtech microplate shaker). The absorbance was measured at 515 nm by a BioRad iMark plate reader (Hercules, CA, USA). The inhibition percentage was calculated according to the formula: $((A_c–A_s)/A_c)$ x 100%, where A_c was absorbance of control solution, A_s was absorbance of samples (NADES or NADES extracts). IC_{50} values were calculated for each sample by regression linear equations which were obtained by plotting the percentage of inhibition against concentrations. Experiments were conducted in three replicates.

Ferric reducing antioxidant power assay

The ability of NADES and NADES extracts to reduce Fe(III) to Fe(II) was assayed using FRAP method, based on Benzi and strain with some modification (Simamora *et al.* 2023). In this assay, the colorless Fe(III) – (2,4,6-tripyrydyl-s-triazine) complex was converted into the blue color Fe(II) – (2,4,6-tripyrydyl-s-triazine) complex by antioxidant compound by way of electron transfer mechanism under an acidic condition. FRAP reagent was prepared by mixing 2,4,6-tris (2-pyridyl)-s-triazine (10 m*M*) in HCl (40 m*M*), $FeCl_3$ (20 m*M*) and acetate buffer (300 m*M*, pH 3.6) in a 1:1:10 ratio. In 20 μL samples serially diluted with water, was added 280 μL of FRAP reagent. The mixture was incubated at 37°C for 30 min at 300 RPM in a shaking incubator (Thermostar BMG Labtech); thereafter the absorbance was read by a BioRad iMark plate reader (Hercules, CA, USA) at 593 nm. Trolox (50 – 800 μmoL/mL) was used to generate a standard curve, and results were presented as a trolox equivalent/gram sample. FRAP activity was compared with ethanol extract. Experiments were conducted in three replicates.

DNA protection assay

The ability of choline chloride-based NADES and their extracts to protect the supercoiled pBR322 DNA against the damaging effects of •OH radical-induced oxidative condition was assessed based on the reported method (Jeong *et al.* 2009). The reaction mixture contained pBR322 DNA (0.5 μG, 5 μL), samples of different concentrations (5 μL),

$FeSO_4$ (1 m*M*, 2 μL) and H_2O_2 (1 m*M*, 2 μL), followed by the addition of phosphate buffer saline (10 m*M*, pH 7.4) to bring the total volume to 17 μL. The reaction mixture was incubated for 30 min at 37°C, and thereafter was stopped with the addition of bromophenol dye (10 m*M* Tris-HCl pH 7.6, 60 m*M* EDTA 0.1% bromophenol blue, 0.1% xylene cyanole FF, 50% glycerol). The mixture which was added with the GelRed staining (Biotium) was loaded onto an agarose gel (0.85% in TAE buffer) and electrophoresed at 60 mV for 60 min. DNA separation was visualized and imaged under UV light using a C238 Azure gel documentation system (Dublin, California, USA) and bands were quantified using ImageJ software. The inhibition of DNA damage was calculated using equation 2:

Inhibition on DNA damage (%) = (sc-DNA with oxidative radicals and samples/sc-DNA without oxidative radicals) × 100 (Equation 2).

Toxicity assay with the use of bacteria

The toxicity of choline chloride-based NADES and extract were investigated using *Escherichia coli* ATCC 33218 and *Staphylococcus aureus* ATCC 25923 as model organisms. The bacterial growth was measured by a real-time bacterial growth assay as previously described (Simamora *et al.* 2023). The bacteria were grown overnight in Luria-Bertani (LB) broth in a shaking incubator (37°C, 300 RPM). In a corning tube, the overnight inoculum (500 μL) was diluted with LB media (15 mL) and added with NADES or NADES extract of *C. xanthorrhiza* samples (50 μL). The tube was placed in a bioreactor RTS 001/001C (BioSan SIA, Riga, Latvia), which was set at 500 RPM. The optical density of the culture was read at 850 nm at 15-min intervals for 20 h. Fresh culture without samples was used as a negative control. Ethanol extract of *C. xanthorrhiza* was used for comparison.

Statistical analysis

Data were processed using IBM SPSS statistics v25. Means between groups were analyzed by one-way ANOVA. Differences among groups were considered significant at the level of $P < 0.05$.

Results

NADES characteristics

Physicochemical properties of CC-NADESs: The physicochemical properties including polarity, viscosity, and density were determined for CC-NADES. Results were presented in Table 2. The polarity of ethanol was included for comparison.

The polarity of choline CC-NADES was empirically measured using a fluorescence solvatochromic probe Nile red. Generally, a slight variation in E_{NR} can be seen in choline chloride-based NADES.

The polarity of CC-NADES in this study is in the following order, CC-CA (pK_a = 3.14) > CC-MA (pK_a = 3.51) > CC-LA (pK_a = 3.86). The highest density was found for CC-CA, followed by CC-MA and CC-LA. The studied NADES were viscous at room temperature (> 0.1 Pa s), in the following order CC-CA>CC-MA>CC-LA. Regarding the density, all the studied NADES showed higher density than water (by more than 15%) and 40% denser than ethanol.

FTIR spectra analysis of NADES

The formation of a eutectic mixture occurs *via* intermolecular H-bonds between precursors of NADES. One typical technique to identify H-bond interactions in a system is FTIR spectroscopy. To this end, all CC-based NADES were scanned by FTIR spectroscopy and the results were compared with those obtained for their starting components

The lactic acid spectrum presented a broad band in the 3600 – 3150 cm^{-1} range, associated with O-H stretching vibration. The C = O stretching of the carboxylic group appeared at 1718 cm^{-1}. The C-O stretching of hydroxyl and carboxylic acid functionalities was observed at 1207 and 1040 cm^{-1}.

Malic acid showed a sharp peak at 3436 cm^{-1} attributed to the O - H stretching vibration. The stretching vibration C = O appeared at 1679 cm^{-1}. Peaks at around 1440 cm^{-1} are related to the C-H bending vibration of the $-CH_2-$. The peak at 1097 is attributed to C - O stretching vibration.

On the spectrum of citric acid, sharp and broad bands at 3492 and 3283 cm^{-1} were attributed to O - H stretching vibrations. The C = O stretching of the carboxylic group appeared at 1742 cm^{-1}.

Choline chloride (CC) spectra presented a sharp band at 3218 cm^{-1} corresponding to the stretching vibration of the O - H group. The peak at 950 cm^{-1} was identified as the stretching of C-N of the quaternary ammonium compound, as also reported by others (Mulia *et al.* 2015; Abou-Taleb *et al.* 2022).

FTIR spectra of CC-LA, CC-MA and CC-CA showed characteristic bands of several functional groups. O-H stretching vibration occurred at a range of 3369 to 3343 cm^{-1}, C-H stretching was observed between 3006 to 2929 cm^{-1}, C=O stretching vibration occurred at a range of 1720 to 1714 cm^{-1} and C-O stretching vibration at ranges 1174 to 1138 cm^{-1}.

Extraction and quantification of xanthorrhizol

This study used all NADES (CC-LA, CC-MA and CC-CA) for extraction of *C. xanthorrhiza*. Extraction conditions were optimized previously for these systems *i.e.*, S/L ratio 1/15, 20 min sonication time, and 25% (v/v) water content in NADES), and CC-MA was demonstrated to obtain the highest amount of xanthorrhizol (Nadia 2022). The same optimized conditions were applied to the NADES studied here.

HPLC analysis showed that CC-MA extract obtained a similar amount of xanthorrhizol than curcuminoids (Fig. 2).

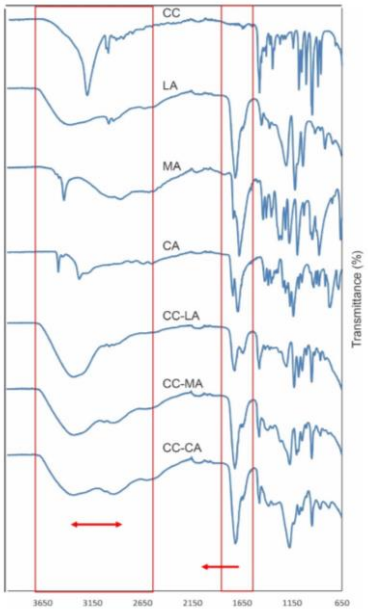

Fig. 1: FTIR analysis of CC-based NADES and the starting components.

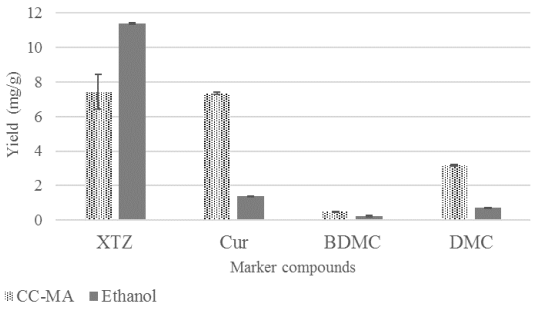

Fig. 2: Yields of extraction by (A) CC-MA and (B) ethanol (96%). XTZ (xanthorrhizol), Cur (curcumin), BDMC (bisdemethoxycurcumin) and DMC (demethoxycurcumin)

The yields obtained were 7.42 ± 0.50, 7.33 ± 0.03, 0.49 ± 0.001 and 3.17 ± 0.03 mg/g for XTZ, Cur, BDMC and DMC, respectively. Whereas, for ethanol extract; the yields were 11.38 ± 0.04, 1.38 ± 0.01, 0.24 ± 0.06 and 0.71 ± 0.03 mg/g, respectively. The chromatograms of each extract can be seen in Fig. 3.

As shown in Fig. 4 A1 and A2, untreated dried rhizome particles show an intact surface that is clustered together (A1 and A2). In contrast, rhizome powder shows numerous microfractures and ruptures after treatment with combined CC-MA and UAE. The particle surface was disintegrated, which can be caused by the penetration of CCMA and ultrasonication. This may indicate an enhanced capability of CC-MA UAE to disintegrate the polysaccharide wall structures of the rhizome. By comparison, the rhizome particles soaked in ethanol maceration did not change appreciably (B1 and B2).

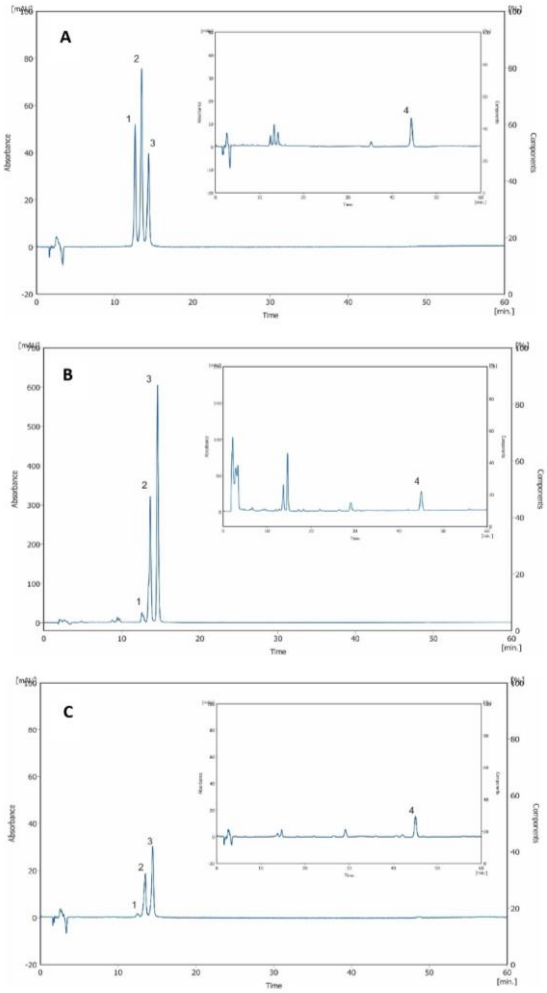

Fig. 3: HPLC chromatograms of (**A**) standard compounds (1) bisdemethoxycurcumin, (2) demethoxycurcumin, (3) curcumin, (4) xanthorrhizol; (**B**) CC-MA extract of *C. xanthorrhiza*; (**C**) Ethanol extract of *C. xanthorrhiza*

Although the particle fragmentation was noticeable (Fig. 4A), the outer surface was preserved, with only slight deterioration.

Bioactivities of CC-NADES extracts

Antioxidant activity: Two methods were applied for measuring antioxidant activities, FRAP assay and DPPH assay. Either by FRAP or DPPH assays, all CC-NADES showed weaker reduction capacity than CC-NADES extracts. CC-NADES extracts showed higher reduction capacity compared to CC-NADES. Although, ethanol extract yielded higher activity than all CC-NADES (Table 3).

DNA protective activity

Upon treatment with CC-NADES (CC-LA, CC-MA and CC-CA) at concentrations from 1.38 to 44.11 mg/mL), the

Table 1: The composition of the studied NADES and their abbreviations

Component 1	Component 2	Mole ratio	NADES abbreviation	Appearance
Choline chloride	lactic acid	1:1	CC-LA	Slightly viscous, transparent
Choline chloride	malic acid	1:1	CC-MA	Slightly viscous, transparent
Choline chloride	citric acid	1:1	CC-CA	Highly viscous, transparent

Table 2: Physicochemical characterization of the studied NADES systems

NADES	Polarity (E_{NR}, kcal mol^{-1})	Viscosity (mPa s)	Density (g cm^{-3})	Appearance
CC-LA	48.25 ± 0.06^{bcd}	20.76	1.15 ± 0.007^{bcd}	Slightly viscous, transparent
CC-MA	47.76 ± 0.04^{ad}	130.20	1.26 ± 0.007^{acd}	Slightly viscous, transparent
CC-CA	47.73 ± 0.08^{ad}	4566.00	1.32 ± 0.004^{abd}	Highly viscous, transparent
Ethanol	52.12 ± 0.00^{abc}	1.88	0.78 ± 0.007^{abc}	

Data are expressed as mean ± SD (n = 3)
Different letters indicate statistically differences, analyzed using a Tukey analysis

Table 3: Antioxidant activity of the studied NADES and extracts of *C. xanthorrhiza*

Samples	FRAP (mmol TE g^{-1} NADES or solvent)*	FRAP (mmol TE g^{-1} NADES extract)*	DPPH (IC_{50}, mg/mL)	DPPH (IC_{50} Extracts, mg/mL)
CC-LA	0.044 ± 0.002^{bcd}	4.99 ± 0.66^{bcd}	69.54 ± 6.90^{c}	47.46 ± 2.00^{bcd}
CC-MA	0.019 ± 0.001^{acd}	0.84 ± 0.05^{ad}	106.97 ± 24.78^{c}	82.82 ± 5.64^{acd}
CC-CA	0.023 ± 0.001^{abd}	0.43 ± 0.02^{ad}	176.94 ± 10.62^{ab}	101.58 ± 6.61^{abd}
Ethanol	0.057 ± 0.00^{abc}	22.7 ± 0.23^{abc}	NM*	0.46 ± 0.03^{abc}

Data are expressed as mean ± SD (n = 3)
Different letters indicate statistically differences, analyzed using a Tukey analysis

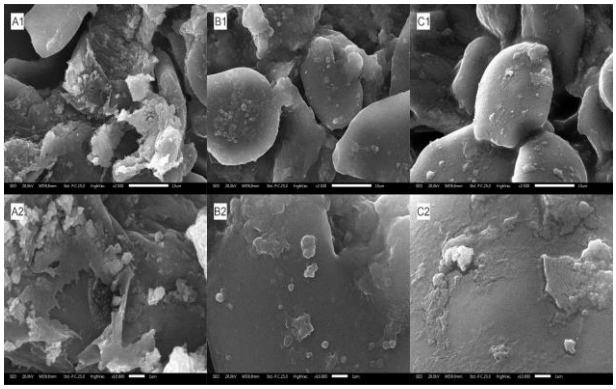

Fig. 4: Scanning electron microscopy images of dried rhizome powder of *C. xanthorrhiza* (A1, A2), powder after extraction by ethanol (B1, B2), and powder after extraction by CC-MA UAE. Images were captured at 2500x and 10000x magnifications

supercoiled form was restored and the relaxed forms (oc-DNA and lin-DNA) disappeared (Fig. 5), dose dependently. The quantification of oc-DNA due to the treatment of studied NADES (CC-LA, CC-MA, and CC-CA) shown in Fig. 5, reveals that NADES were effective in protecting DNA against damage caused Fenton reagents. Restored DNA reached 60 and 70% in the presence of CC-MA and CC-CA at 22.06 and 44.11 mg/mL. At these concentration levels, CC-MA and CC-CA suppressed the formation of oc-DNA, amounting to 50 and 30% of oc-DNA for CC-MA. The addition of CC-CA decreases oc-DNA to 70 and 50% of oc-DNA. In comparison, CC-LA was able to protect plasmid DNA more strongly. Higher increases in native DNA were observed for CC-LA, obtaining 70 and 80% at 22.06 and 44.11 mg/mL, whereas at these concentrations, oc-DNA was reduced, to only 30 and 20%.

In the case of CC-NADES extracts, they showed more effective protection against DNA damage than CC-NADES. For example, extracts of CC-MA at 22.06 and 44.11 mg/mL gave retention of sc-DNA by 70 and 80%. CC-CA restored sc-DNA to 45 and 70% at 22.06 and 44.11 mg/mL, respectively. As in CC-LA, treatment of CC-LA extract resulted in 70 and 90% of sc-DNA, suggesting a condition almost like untreated plasmid DNA. The fragmentation of DNA was decreased, leaving only 30 and 20% of oc-DNA.

For comparison, ethanol extract of *C. xanthorrhiza* showed strong protective activity against OH-induced pBR322 DNA damage. However, the ethanol extracts inhibited DNA damage more than NADES extracts, with similar protective activity was obtained at a much lower concentration range (0.037 - 0.59 mg/mL).

Toxicity profile of CC-NADES against *E. coli* and *S. aureus*

Toxicity profile of CC-NADES against *E. coli:* The bacterial growth curves of *E. coli* in the presence of choline chloride (CC)-based NADES and extract are shown in Fig. 6 and presented as incubation time versus optical density at 850 nm. The control solution (culture media with no NADES) shows expected growth, with a short lag phase (adaption time) lasting only for a few min. High exponential growth followed the first growth phase, as demonstrated by the steep slope. Among the investigated NADES, only CC-CA completely inhibited *E. coli*, representing the high toxicity of CC-CA on *E. coli*. On the other hand, CC-LA and CC-MA still allowed

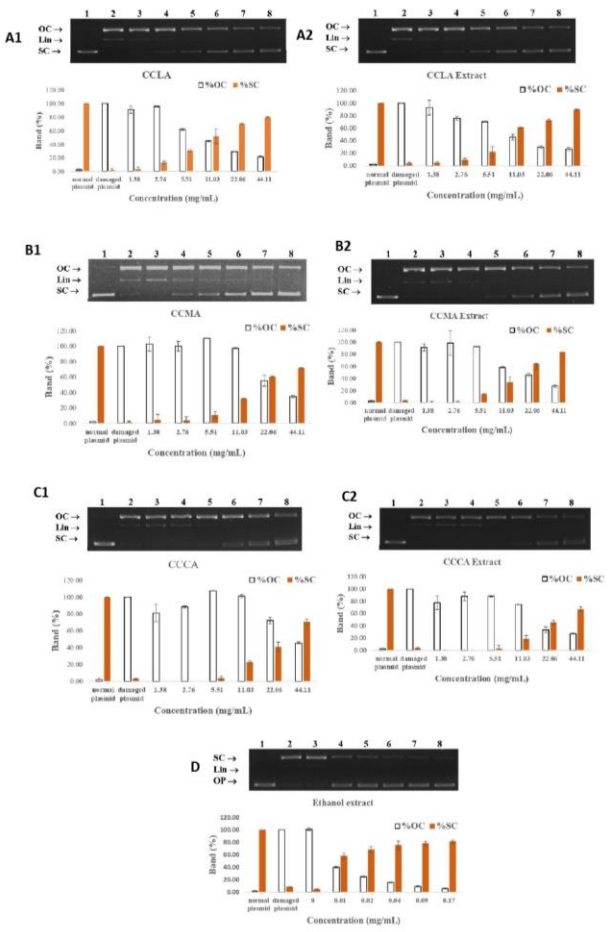

Fig. 5: DNA protection effect of (A1-2) CC-LA and (B1-2) CC-MA and (C1-2) CC-CA and their respective extract, and (D) Ethanol extract. Lanes 1 and 2 are pBR322 DNA in the absence and presence of FeSO4/H2O2, respectively. Lanes 3 – 8 are pBR322 DNA treated with varying concentrations of samples. Underneath the agarose gel figure is the quantification of bands for each sample. Results are presented as mean ± SD from two repeats. OC: open circular conformation, Lin: linier, SC: supercoiled conformation

bacterial growth, although the inhibition effect was observed. In addition, lower yields at the stationary and prolonged lag phases were observed for *E. coli* growth, indicative of *E. coli* inhibition. *E. coli* growth was inhibited with the addition of CC-LA. A prolonged adaption time (lag phase) and low growth rate were observed, as demonstrated by the shallower slope. This curve suggests inhibition on *E. coli* growth. CC-MA appeared more toxic to *E. coli* than CC-LA. CC-MA significantly reduced the growth of *E. coli*. Although similar lag phase time and growth rate to CC-LA were observed, the final maximum OD of CC-MA culture was lower than culture supplemented by CC-LA, indicating that CC-MA is more toxic than CC-LA. In contrast to CC-LA and CC-MA, treatment of CC-CA on *E. coli* prevented the growth of *E. coli*.

For all the studied NADES, the toxicity effect on *E. coli* was lower when we treated the culture media with CC-based extracts of *C. xanthorrhiza*. Unlike CC-LA, adding CC-LA extract resulted in a diauxic growth of *E. coli*. A higher yield was observed, suggesting the extract's lower toxicity to *E. coli* than CC-LA. The *C. xanthorrhizol* CC-MA extract had a similar yield to CC-MA, although the CC-MA extract had a shorter lag phase. This result highlights the inhibition of CC-MA extract on *E. coli*. Unlike with CC-CA, growth was still observed, even though we obtained a low yield when we treated the culture media with CC-CA extract. By comparison, treatment with ethanol or ethanol extract of *C. xanthorrhiza* did not affect *E. coli*. This result indicates the cellular tolerance of *E. coli* to the extract.

Toxicity profile of CC-NADES against *S. aureus*

The studied NADES and their respective extracts were relatively safe for *S. aureus* (Fig. 7). A short adaptation time similar to the control was observed for all studied NADES and their extracts, except for CC-MA and CC-MA extract. All NADES showed lower growth rates and yields than the control. Although growth in the presence of CC-MA was observed, this NADES inhibited *S. aureus* growth. CC-MA prolonged the lag phase and slowed the growth rate of *S. aureus*. In addition, the culture reached the stationary phase after 12 h, compared to the growth profiles of other NADES (between 2 and 7 h). This result indicates that CC-MA prevented *S. aureus* growth. A comparison to the CC-MA extract was done. As with CC-MA, CC-MA extract had a similar yield at the stationary phase, although this phase was attained after a prolonged exponential phase, like CC-MA.

Discussion

Inherent properties of the studied NADES, such as polarity, viscosity, and density affect the extraction performance of NADES towards xanthorrhizol. Therefore, suitable NADES should be used to enhance extraction. Solvent polarity is an important indicator of solvent strength which affects affinity towards various polar and semipolar phytocompounds. The polarity of NADES is assessed based on the λ_{max} response of the Nile red in the presence of NADES. The charge transfer mechanism occurring in the probe can be associated with the hydrogen bond ability of NADES to the Nile red probe (Pandey *et al.* 2014). More polar solvents shift the λ_{max} to a longer wavelength, which leads to lower E_{NR} by equation 1. Results in Table 2 show that all NADES were more polar than ethanol. However, among the studied NADES, the polarity was slightly different. The slight variation observed can be associated with the acid strength of the HBD components, *i.e.*, CC-CA (pK_a = 3.14), CC-MA (pK_a = 3.51), and CC-LA (pK_a = 3.86).

According to Eq. 1, the experimental values of E_{NR} for CC-CA yielded a value of 47.73. This value differs only by 0.3% from the value reported previously

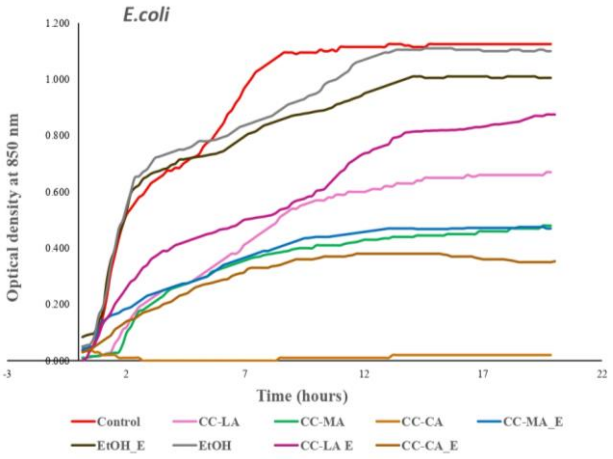

Fig. 6: Growth curves of *E. coli* treated with choline chloride-based NADES (lactic acid, malic acid and citric acid) and *C. xanthorrhiza* extracts in NADES. Control (red line) corresponds to culture lacking NADES or extracts. Ethanol and ethanol extract were measured for comparison

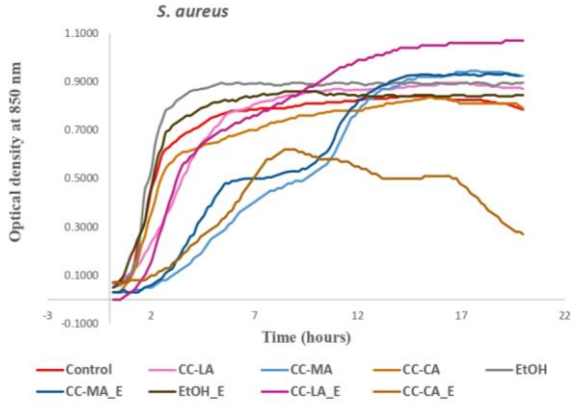

Fig. 7: Growth curves of *E. coli* treated with choline chloride-based NADES (lactic acid, malic acid and citric acid) and *C. xanthorrhiza* extracts in NADES. Control (red line) corresponds to culture lacking NADES or extracts. Ethanol and ethanol extract were measured for comparison

(Craveiro *et al.* 2016). CA which contains three carboxylic acid functionalities, compared to only two and one groups for MA and LA, respectively, is the strongest acid. In addition, more -OH groups in HBA and HBD also increases the polarity of the synthesized NADES, as the -OH group can act as H-bond binding sites, to produce stronger interaction and more polar NADES (Jurić *et al.* 2021). Accordingly, its combination with choline chloride brings about the most polar choline chloride-based NADES, followed by CC-MA and CC-LA. Ethanol yielded the highest E_{NR} value (51.54), implying the least polar solvency. This result is reasonable since ethanol only has one -OH group.

Density can be explained by the hole theory, which assumes that NADES are composed of holes and vacancies (Abbott *et al.* 2004). Accordingly, the physical properties of NADES, including density, depend on the molecular organization and packing of NADES components. When CC was mixed with HBD, the average hole radius was decreased and results in an increase in NADES density (Lee *et al.* 2021). With more -OH groups in CA, CC-CA may form more hydrogen bond interactions between components, resulting in more compact molecular organization, thus higher density NADES.

The viscosity of NADES originates from extensive H-bond interactions between CC and HBDs. Compared to MA and LA, CA—with its three carboxylic acids and one -OH functional group—presents maximum H-bond interactions with CC, resulting in highly viscous NADES. Other factors may contribute to the highly viscous nature of NADES, *i.e.*, large ion size and small void volume (Qin *et al.* 2020). In addition to H-bond formation, electrostatic and Van der Waals interactions also cause high viscosity (Qin *et al.* 2020).

Confirmation of the formation of H-bond between the starting components of NADES can be seen from analysis of FTIR spectroscopy. It can be observed that FTIR spectra of CC-based NADES maintained characteristic bands of the starting constituents (Fig. 1). The preservation of the constituents' bands indicates that intermolecular forces were the driving force in the formation of NADES (Mjalli 2016). In CC spectrum, O-H stretching vibration of choline chloride was observed at 3218 cm^{-1}. This band was observed as a broad band at longer wavenumbers in all CC based-NADES, *i.e.*, CC-LA, CC-MA and CC-CA at 3341, 3343 and 3369 cm^{-1}, respectively. The wide band observed and the band shifting strongly confirms the formation of hydrogen bonds between chloride anion and the hydroxyl group of organic acids (Doldolova *et al.* 2021). It is noticeable that the breadth of this band differs among CC-LA, CC-MA and CC-CA, with increasing order. The wider band at this wavelength may suggest that HBA (CC) and HBD had more hydrogen bond interaction, as also observed by other researchers (Alioui *et al.* 2022). The extensive hydrogen bond network present in CC-CA is also seen in its high viscosity value (Table 2). With regard to the spectra of hydrogen bond donors, C=O vibration of the carboxylic group was observed at longer wavelength in CC-LA, CC-MA, and CC-CA (1718 to 1720, 1679 to 1720 and 1694 to 1714 cm^{-1}, respectively). The red shift of C=O stretching has been reported to be associated with the hydrogen bond interaction between carbonyl group and hydroxyl groups (Phaechamud *et al.* 2016). It is also worth noting that an additional characteristic peak that originating from CC (950 cm^{-1}) appeared in all NADES, which is attributed to $C\text{-}N^{+}$ stretching vibration (Abou-Taleb *et al.* 2022).

When used for extraction, highly viscous solvents such as NADES are difficult to disperse, thus restricting mass transfer and hindering efficient mass transfer and diffusivity. In addition, viscous liquid requires higher energy consumption for mixing or pumping in the preparation and separation steps. The results were low extraction efficiency.

However, highly viscous NADES, such as those observed in CC-based NADES, may be a desired characteristic for extraction since it allows stable molecular interaction between NADES and the target compounds (Mitar *et al.* 2019). In addition, viscous solvents may aid extraction in conjunction with ultrasonication. Using viscous solvents for ultrasound-assisted extraction increases the cavity threshold for bubble implosion. Viscous solvents also require more ultrasonic energy to initiate mechanical vibration. However, the low vapor pressure of NADES causes a more intense bubble collapse, leading to a more effective impact on the destruction of plant cell walls.

Extraction yields by using CC-MA could be due to the synergistic effect of using CC-MA as an extraction solvent and ultrasonication during extraction. SEM images were taken to examine the extraction process and its possible mechanisms. The morphology of rhizome surface treated with CC-MA showed cracking and loose structures (Fig. 4C). This may indicate an enhanced capability of CC-MA UAE to disintegrate the polysaccharide wall structures of the rhizome. In comparison, rhizome treated with ethanol and without treatment showed little alterations on the surface morphology, as seen in intact and smooth surface (Fig. 4A and B). Others have reported the combined effect of NADES and ultrasonication in enhancing extraction. Fu *et al*. (2021) compared extraction by CC-MA and CC-MA combined with UAE to extract phenolic compounds from *Carya cathayensis* and found that CC-MA coupled with ultrasonication caused more fragmentation and ruptured surface compared to treatment with only CC-MA (Fu *et al.* 2021). Although ethanol extract obtained higher yield of XTZ, it should be noted however, that extraction using CC-MA was achieved in 20 min sonication time, far shorter than a few days extraction time in ethanol maceration. Further, the use of ethanol as extraction solvent brings about health concerns due to its flammability. On the other hand, by having low vapor pressure, the use of CC-MA for extraction negates this negative effect.

Similar to other solvent systems, ultrasonic waves induce mechanical vibration mediated by CC-MA, leading to the formation of cavitation bubbles. Successive propagation causes the cavitation bubbles to exceed the threshold leading to implosion that creates instantaneous local high pressure and high temperature. These mechanical effects generate shock waves and microjets that are responsible for the loosening and disintegration of plant material (Tao and Sun 2015). Although viscous solvent such as NADES requires higher ultrasound intensity to reach the cavitation bubble threshold, however, due to their low vapor pressure, the collapse of the cavitation bubbles brings about a more violent agitation that enhances extraction (Zhang *et al.* 2018). All these characteristics of NADES may be the contributing factors that increase extraction efficiency.

The antioxidant activity of NADES is still poorly reported, but several reports are available (Radošević *et al.* 2016; Jurić *et al.* 2021). Previous research has suggested that the individual components of NADES, such as their organic acids, exhibit different modes of antioxidant activity. The present study evaluated the antioxidant activity of CC-based NADES, and their extracts of *C. xanthorrhiza* were evaluated with FRAP and DPPH radical scavenging assays.

The observed antioxidant activity of NADES by FRAP assay indicates that NADES can contribute to the electron-donating ability. However, the studied NADES generally showed weak activity compared to ethanol. Although organic acid components (LA, MA and CA) are known antioxidants due to their ability to donate electrons or protons, our results showed weak reduction activity for the acid-containing NADES. It is likely that upon incorporation of CC with the organic acids in eutectic mixtures, charge delocalization of the anions through H-bond interaction with CC may reduce the ability of the organic acids to donate electrons. Jurić *et al.* (2021) have reported reducing the capacity of CC-based NADES with LA, MA, and CA (1:1, 20% water). However, their results cannot be directly compared to ours because of the difference in the methodology and water content used in the CC-based NADES. The higher reduction capacity of NADES extract compared to NADES suggests the contribution of the extracted compounds to the reducing power. CC-LA extract showed the highest activity, followed by CC-MA extract > CC-CA extract. Notably, ethanol extract showed the highest reduction capacity.

The radical scavenging activity of the studied NADES is expected because the forming components (LA, MA and CA) are well-known radical scavenging compounds (Tang *et al.* 2013). The radical scavenging activity of NADES extracts was stronger than NADES solvent (Table 3), which is plausible due to the different antioxidant compounds extracted by each NADES from *C. xanthorrhiza*. It has been reported that the proton/electron donating ability correlates with the presence of the -OH groups of antioxidant molecules (Mensor *et al.* 2001), that could be associated with the -OH groups attached to diarylheptanoids or terpenoids known to be present in *C. xanthorhiza* (Awin *et al.* 2016). It is worth noting that a similar pattern was observed for the radical scavenging activity of NADES and their extracts. NADES containing CC-LA presented the strongest activity, followed by CC-MA and CC-CA. By comparison, ethanol extract showed the strongest activity as observed by FRAP assay.

The protection effect of CCLA, CCMA and CCCA and their extracts against DNA oxidative damage was evaluated by an *in vitro* DNA cleavage assay using pBR322 plasmid DNA. Conversion of supercoiled plasmid DNA into relaxed forms (open circular and linear forms) has been used as an index for DNA damage (Kumar *et al.* 2013; Huang *et al.* 2022). In this assay, $FeSO_4/H_2O_2$ was applied to induce OH radicals to cause oxidative damage to pBR322 plasmid DNA.

To date, very limited study has reported the DNA protective effect of NADES. The DNA protective effect of

NADES is likely caused by the radical scavenging activity and reducing capacity of NADES as shown in Table 3. In addition, the ability of organic acids (LA, MA and CA) to chelate Fe(II), thus inhibiting the Fenton reaction, may also contribute to the DNA protective effect of NADES.

Studies reported that extracts rich in polyphenols were able to protect pBR322 plasmid from OH radical's damage (Yates *et al.* 2019; Moyo *et al.* 2020; Huang *et al.* 2022). In particular, several studies have reported the protective effects of curcumin against OH radical-induced damage on pBR322 plasmid (Kong *et al.* 2009). As reported by various studies, the activity of antioxidants to influence diseases closely correlates with their ability to reduce DNA damage and mutagenesis (Beetch *et al.* 2020). Oxidative DNA damage caused by excessive ROS (such as OH radicals) causes cellular damage. It is known that irreparable DNA damage is involved in carcinogenesis, aging, and other degenerative diseases (Tiwari and Wilson 2019). Findings in the present study may indicate potential application of NADES extract of *C. xanthorrhiza* for the prevention of health risks by DNA oxidative damage, such as aging and cancer.

The toxicity effect of the studied NADES was tested based on microbial bioassay method using a Gram-negative (*E. coli*) and a Gram-positive bacterium (S. aureus). Microbial toxicity assay provides a rapid and inexpensive assessment because of the short life cycle. In addition, microorganisms are known to be sensitive to different toxicants such as heavy metals, phenolics, organic pollutants and industrial wastes (Hayyan *et al.* 2016). *E. coli* and *S. aureus* are an ideal starting point for toxicity evaluation of NADES due to their relevance in human and animal health and biotechnology (Young *et al.* 2012; Fu *et al.* 2013). In this study, the time kill assay was employed for this purpose which measures real time monitoring of bacterial growth, thus provides dynamic analysis of bacterial behavior in the presence of toxicants.

As other researchers have reported, a diauxic growth curve (Fig. 6) was observed for the control solution *i.e*., *E.coli* without inhibitiors (Torregrosa-Crespo *et al.* 2020). The diauxic form can result from (i) the changes in the physicochemical parameters of the culture media during the incubation period, or (ii) can be induced by the use of two different substrates (Torregrosa-Crespo *et al.* 2020). CC-based NADES and their respective extracts gave different toxicity responses than the controls.

Results within this study showed that CC-based NADES showed different toxicity behavior on *E. coli*. Regarding the acids, the toxicity follows the order of CC-CA > CC-MA > CC-LA. This order did not correlate with the lipophilicity of the acids (log K_{ow} of LA, MA, and CA are -0.65, -1.26 and -1.67, respectively). Protonated (thus uncharged) weak organic acids are more lipophilic and can permeate lipid bilayers, which results in cytoplasmic acidification (Lund 2020). In this study, each NADES (50 µL) was added to LB media (15 mL), increasing the system's pH to 5-6 for malic acid and citric acid containing NADES and 6-7 for lactic acid containing NADES. The abundance of water surrounding NADES suggests that the hydrogen bond network in NADES may partially disintegrate and release the NADES components lactate, malate, and citrate anions. The chelation of metal ions mediates the antibacterial activity of citric acid (Burel *et al.* 2021) and stabilization of the negatively charged lipopolysaccharide layer of Gram-negative bacteria is due to the presence of divalent metal ions. Therefore, the chelation of metal ions by lactate, malate, and citrate may weaken the bacterial membrane.

The above findings highlight that *E. coli*, a Gram-negative bacterium, was more susceptible to the studied CC-based NADES and NADES extracts than to *S. aureus* (a Gram-positive bacterium). These results confirm previous studies by Hou *et al.* (2013) and Wen *et al.* (2015). They found that choline chloride-based NADES were more reactive to the Gram-negative bacteria. Although Gram-negative bacteria possess an extra outer lipopolysaccharide membrane on the cell wall and are thus less susceptible to toxicity, our results suggest their toxicity toward *E. coli*. Zhao *et al.* (2015) reported that all acids containing CC-DES inhibited Gram-negative and Gram-positive bacteria, including *E. coli* and *S. aureus*. These toxicity effects were induced by acids in CC-based DES. However, different toxicity profiles were obtained in this study, in which CC-based NADES with LA, MA and CA exhibited slight toxicity on *S. aureus*. In the present study, we used different methods to obtain these results, in which a real time bacterial growth assay was used. By this method, the extent of toxicity can be better described in terms of growth rate, yields, and adaptation time by real-time monitoring of bacterial growth. In addition, using liquid media instead of solid culture media (disk test) presents more accurate results, as this approach determines the diffusivity of highly dense and viscous NADES, such as those investigated in this study.

Conclusion

In this study, CC-based NADES with LA, MA and CA were applied for the extraction of xanthorrhizol and curcuminoids. CC-based NADES showed similar polarity; however, their density and viscosity were varied, related to the acid properties of the organic acids. The FTIR spectra results proved the H-bonds formed between the starting components, which led to the formation of the eutectic mixture. The HPLC analysis showed that UAE-CC-MA gave comparable xanthorrhizol and curcuminoids yields to ethanol. Based on bacterial toxicity tests, CC-based NADES and their respective extracts were benign to *S. aureus* and caused different toxicity against *E. coli*. All CC-based NADES protected DNA from OH radical-induced damage. The protective activity was more robust in pBR322 treated with NADES extracts of *C. xanthorrhiza*, which indicates the contributing role of the extracted bioactive compounds in NADES. The DNA protective activity and low toxicity of

CC-based solvents and extracts suggest the potential to use these extracts in food and pharmaceutical preparations.

Acknowledgments

AS was thankful to Krida Wacana Christian University, for providing her PhD program scholarship.

Author Contributions

AS: conceptualization, methodology, investigation, writing original draft, and editing. KHT: conceptualization, methodology, review and editing, supervision. HS: methodology, supervision, review. RAN: Supervision, review. AM: conceptualization, methodology, supervision, resources, funding acquisition, review and editing. All authors agree to the final version of the manuscript.

Conflicts of Interest

The authors report there is no competing interest to declare.

Funding Source

This work was supported by The Ministry of Research and Technology and Higher Education of the Republic of Indonesia for PKN/PK 2023, under Grant (NKB-1084/UN2.RST/HKP.05.00/2023) for funding the research materials; The Institute for Research and Community Service (Lembaga Penelitian dan Pengabdian pada Masyarakat – LPPM) Krida Wacana Christian University (Grant number 02/UKKW/LPPM-FKIK/LIT/05/2023) for the use of the research facilities and some of the spectroscopy analysis.

References

Abbott AP, D Boothby, G Capper, DL Davies, RK Rasheed (2004). Deep eutectic solvents formed between choline chloride and carboxylic acids: Versatile alternatives to ionic liquids. *J Amer Chem Soc* 126:9142–9147

Abou-Taleb NH, DT El-Sherbiny, NM El-Enany, HI El-Subbagh (2022). A new grey relational analysis application in analytical chemistry: Natural deep eutectic solvent as a green extractant for HPLC determination of lamotrigine in plasma. *Microchem J* 172:106918

Ahmad I, AM Syakfanaya, A Azminah, FC Saputri, A Mun'im (2021). Optimization of betaine-sorbitol natural deep eutectic solvent-based ultrasound-assisted extraction and pancreatic lipase inhibitory activity of chlorogenic acid and caffeine content from robusta green coffee beans. *Heliyon* 7:e07702

Alioui O, W Sobhi, M Tiecco, IM Alnashef, A Attoui, A Boudechicha, K Kumar Yadav, AM Fallatah, N Elboughdiri, BH Jeon, Y Benguerba (2022). Theoretical and experimental evidence for the use of natural deep eutectic solvents to increase the solubility and extractability of curcumin. *J Mol Liq* 359:119149

Awin T, A Mediani, Maulidiani, K Shaari, SMM Faudzi, MAH Sukari, NH Lajis, F Abas (2016). Phytochemical profiles and biological activities of *Curcuma* species subjected to different drying methods and solvent systems: NMR-based metabolomics approach. *Indust Crops Prod* 94:342–352

Beetch M, S Harandi-Zadeh, K Shen, K Lubecka, DD Kitts, HM O'Hagan, B Stefanska (2020). Dietary antioxidants remodel DNA methylation patterns in chronic disease. *Braz J Pharmacol* 177:1382–1408

Bi Y, X Chi, R Zhang, Y Lu, Z Wang, Q Dong, C Ding, R Yang, L Jiang (2020). Highly efficient extraction of mulberry anthocyanins in deep eutectic solvents: Insights of degradation kinetics and stability evaluation. *Innov Food Sci Emerg Technol* 66:102512

Burel C, A Kala, L Purevdorj-Gage (2021). Impact of pH on citric acid antimicrobial activity against Gram-negative bacteria. *Lett Appl Microbiol* 72:332–340

Craveiro R, I Aroso, V Flammia, T Carvalho, MT Viciosa, M Dionísio, S Barreiros, RL Reis, ARC Duarte, A Paiva (2016). Properties and thermal behavior of natural deep eutectic solvents. *J Mol Liq* 215:534–540

Cui Q, JZ Liu, LT Wang, YF Kang, Y Meng, J Jiao, YJ Fu (2018). Sustainable deep eutectic solvents preparation and their efficiency in extraction and enrichment of main bioactive flavonoids from sea buckthorn leaves. *J Clean Prod* 184:826–835

Doldolova K, M Bener, M Lalikoğlu, YS Aşçı, R Arat, R Apak (2021). Optimization and modeling of microwave-assisted extraction of curcumin and antioxidant compounds from turmeric by using natural deep eutectic solvents. *Food Chem* 353:129337

Florindo C, LC Branco, IM Marrucho (2019). Quest for green-solvent design: From hydrophilic to hydrophobic (deep) eutectic solvents. *Chem Sus Chem* 12:1549–1559

Fu M, C Qin, W Li, Y Yan, L Zeng, X Yang (2013). Effect of glucosamine and chitooligomer on the toxicity of arsenite against *Escherichia coli*. *Carbohydr Polym* 91:390–393

Fu X, D Wang, T Belwal, Y Xu, L Li, Z Luo (2021). Sonication-synergistic natural deep eutectic solvent as a green and efficient approach for extraction of phenolic compounds from peels of *Carya cathayensis* Sarg. *Food Chem* 355:129577

Hayyan M, YP Mbous, CY Looi, WF Wong, A Hayyan, Z Salleh, O Mohd-Ali (2016). Natural deep eutectic solvents: Cytotoxic profile. *Springer Plus* 5:913

Hou XD, QP Liu, TJ Smith, N Li, MH Zong (2013). Evaluation of toxicity and biodegradability of cholinium amino acids ionic liquids. *PLoS One* 8:e59145

Huang H, Y Zhu, X Fu, Y Zou, Q Li, Z Luo (2022). Integrated natural deep eutectic solvent and pulse-ultrasonication for efficient extraction of crocins from gardenia fruits (*Gardenia jasminoides* Ellis) and its bioactivities. *Food Chem* 380:132216

Jeong JB, JH Park, HK Lee, SY Ju, SC Hong, RK Lee, GY Chung, JH Lim, HJ Jeong (2009). Protective effect of the extracts from *Cnidium officinale* against oxidative damage induced by hydrogen peroxide via antioxidant effect. *Food Chem Toxicol* 47:525–529

Jurić T, D Uka, BB Holló, B Jović, B Kordić, BM Popović (2021). Comprehensive physicochemical evaluation of choline chloride-based natural deep eutectic solvents. *J Mol Liq* 343:116968

Kesehatan RIK (2017). *Farmakope Herbal Indonesia*, 2nd edn. Jakarta, Kementerian Kesehatan Republik Indoensia

Kong Y, W Ma, X Liu, Y Zu, Y Fu, N Wu, L Liang, L Yao, T Efferth (2009). Cytotoxic activity of curcumin towards CCRF-CEM leukemia cells and its effect on DNA damage. *Molecules* 14:5328–5338

Kumar GP, K Navya, EM Ramya, M Venkataramana, T Anand, KR Anilakumar (2013). DNA damage protecting and free radical scavenging properties of *Terminalia arjuna* bark in PC-12 cells and plasmid DNA. *Free Rad Antioxid* 3:35–39

Lee KM, JY Hong, WY Tey (2021). Combination of ultrasonication and deep eutectic solvent in pretreatment of lignocellulosic biomass for enhanced enzymatic saccharification. *Cellulose* 28:1513–1526

Lund PA, D De Biase, O Liran, O Scheler, NP Mira, Z Cetecioglu, EN Fernández, S Bover-Cid, R Hall, M Sauer, C O'Byrne (2020). Understanding how microorganisms respond to acid pH is central to their control and successful exploitation. *Front Microbiol* 11:556140

Mangunwardoyo W, T Usia (2012). Antimicrobial and identification of active compound *Curcuma xanthorrhiza* Roxb. *Intl J Basic Appl Sci* 12:69–78

Mensor LL, FS Menezes, GG Leitão, AS Reis, TCD Santos, CS Coube, SG Leitao (2001). Screening of Brazilian plant extracts for antioxidant activity by the use of DPPH free radical method. *Phytother Res* 15:127–130

Mitar A, M Panić, JP Kardum, J Halambek, A Sander, KZ Kucan, IR Redovnikovic, K Radosevic (2019). Physicochemical properties, cytotoxicity, and antioxidative activity of natural deep eutectic solvents containing organic acid. *Chem Biochem Eng Q* 33:1–18

Mjalli FS (2016). Novel amino acids based ionic liquids analogues: Acidic and basic amino acids. *J Taiwan Inst Chem Eng* 61:64–74

Moyo, SM, JC Serem, MJ Bester, V Mavumengwana, E Kayitesi (2020). The impact of boiling and *in vitro* human digestion of *Solanum nigrum* complex (Black nightshade) on phenolic compounds bioactivity and bioaccessibility. *Food Res Intl* 137:109720

Mulia K, E Krisanti, F Terahadi, S Putri (2015). Selected natural deep eutectic solvents for the extraction of a Mangostin from Mangosteen (*Garcinia Mangostana* L.) pericarpp. *Intl J Technol* 6:1211–1220

Nadia B (2022). Extraction of Javanese turmeric rhizomes (*Curcuma xanthorrhiza* Roxb) with choline chloride and organic acid-based natural deep eutectic solvents by ultrasound assisted-extraction, *Bachelor degree*. Depok, Universitas Indonesia

Nurcholis W, AA Munshif, L Ambarsari (2018). Xanthorrhizol contents, α-glucosidase inhibition, and cytotoxic activities in ethyl acetate fraction of *Curcuma zanthorrhiza* accessions from Indonesia. *Rev Bras Farmacogn* 28:44–49

Oon SF, M Nallappan, TT Tee, S Shohaimi, NK Kassim, MSF Sa'ariwijaya, YH Cheah (2015). Xanthorrhizol: A review of its pharmacological activities and anticancer properties. *Cancer Cell Intl* 15:100–116

Pandey A, R Rai, M Pal, S Pandey (2014). How polar are choline chloride-based deep eutectic solvents? *Phys Chem Chem Phys* 16:1559–1568

Patil SS, A Pathak, VK Rathod (2021). Optimization and kinetic study of ultrasound assisted deep eutectic solvent based extraction: A greener route for extraction of curcuminoids from *Curcuma longa*. *Ultrason Sonochem* 70:105267

Phaechamud T, S Tuntarawongsa, P Charoensuksai (2016). Evaporation behavior and characterization of eutectic solvent and ibuprofen eutectic solution. *AAPS Pharm Sci Tech* 17:1213–1220

Qin H, X Hu, J Wang, H Cheng, L Chen, Z Qi (2020). Overview of acidic deep eutectic solvents on synthesis, properties and applications. *Green Ener Environ* 5:8–21

Radošević, K, N Ćurko, VG Srček, MC Bubalo, M Tomašević, KK Ganić, IR Redovniković (2016). Natural deep eutectic solvents as beneficial extractants for enhancement of plant extracts bioactivity. *LWT-Food Sci Technol* 73:45–51

Rahmat E, J Lee, Y Kang (2021). Javanese turmeric (*Curcuma xanthorrhiza*. Roxb): Ethnobotany, phytochemistry, biotechnology, and pharmacological activities. *Evid Based Compl Altern Med* 2021:9960813

Salea R, E Widjojokusumo, B Veriansyah, RR Tjandrawinata (2014). Optimizing oil and xanthorrhizol extraction from *Curcuma xanthorrhiza* Roxb. rhizome by supercritical carbon dioxide. *J Food Sci Technol* 51:2197–2203

Simamora A, KH Timotius, H Setiawan, MY Putra, A Mun'im (2023). Natural deep eutectic solvent extraction of xanthorrhizol and curcuminoids from *Curcuma xanthorrhiza* Roxb and simultaneous determination by high-performance liquid chromatography. *J Pharm Pharmacogn Res* 11:1056–1071

Simamora A, KH Timotius, MB Yerer, H Setiawan, A Mun'im (2022). Xanthorrhizol, a potential anticancer agent, from *Curcuma xanthorrhiza* Roxb. *Phytomedicine* 105:124359.

Tang X, J Liu, W Dong, P Li, L Li, C Lin, Y Zheng, J Hou, D Li (2013). The Cardioprotective effects of citric acid and L-malic acid on myocardial ischemia/reperfusion injury. *Evid Based Compl Altern Med* 2013:820695

Tao Y, DW Sun (2015). Enhancement of food processes by ultrasound: A review. *Crit Rev Food Sci Nutr* 55:570–594

Tiwari V, DM Wilson (2019). DNA damage and associated DNA repair defects in disease and premature aging. *Amer J Hum Genet* 105:237–257

Torregrosa-Crespo J, X Marset, G Guillena, DJ Ramón, RM Martínez-Espinosa (2020). New guidelines for testing "Deep eutectic solvents" toxicity and their effects on the environment and living beings. *Sci Total Environ* 704:135382

Wen Q, JX Chen, YL Tang, J Wang, Z Yang (2015). Assessing the toxicity and biodegradability of deep eutectic solvents. *Chemosphere* 132:63–69

Yates K, F Pohl, M Busch, A Mozer, L Watters, A Shiryaev. PKT Lin (2019). Determination of sinapine in rapeseed pomace extract: Its antioxidant and acetylcholinesterase inhibition properties. *Food Chem* 276:768–775

Young, YF, HJ Lee, YS Shen, SH Tseng, CY Lee, NH Tai, HY Chang\ (2012). Toxicity mechanism of carbon nanotubes on *Escherichia coli*. *Mater Chem Phys* 134:279–286

Zhang QW, LG Lin, WC Ye (2018). Techniques for extraction and isolation of natural products: A comprehensive review. *Chin Med* 13:20

Zhao BY, P Xu, FX Yang, H Wu, MH Zong, WY Lou (2015). Biocompatible deep eutectic solvents based on choline chloride: Characterization and application to the extraction of rutin from *Sophora japonica*. *ACS Sustain Chem Eng* 3:2746–2755